Calculation of a Gap Restoration in the Membrane Skeleton of the Red Blood Cell: Possible Role for Myosin II in Local Repair

C. Cibert,* G. Prulière,# C. Lacombe,§ C. Deprette,¶ and R. Cassoly¶

*Laboratoire de Biologie du Développement, Institut Jacques Monod, UMR 7592, CNRS, Universités Paris VI et Paris VII, F-75005 Paris; #URA671 CNRS Station de Zoologie Marine, BP28 F-06234 Villefranche-sur-Mer Cedex; §Laboratoire de Bioactivation des Peptides, Institut Jacques Monod, UMR 7592, CNRS, Universités Paris VI et Paris VII, F-75005 Paris; and ¶Laboratoire de Biologie Cellulaire des Membranes, Institut Jacques Monod, UMR 7592, CNRS, Universités Paris VI et Paris VII, F-75005 Paris, France

ABSTRACT Human red blood cells contain all of the elements involved in the formation of nonmuscle actomyosin II complexes (V. M. Fowler. 1986. *J. Cell. Biochem.* 31:1–9; 1996. *Curr. Opin. Cell Biol.* 8:86–96). No clear function has yet been attributed to these complexes. Using a mathematical model for the structure of the red blood cell spectrin skeleton (M. J. Saxton. 1992. *J. Theor. Biol.* 155:517–536), we have explored a possible role for myosin II bipolar minifilaments in the restoration of the membrane skeleton, which may be locally damaged by major mechanical or chemical stress. We propose that the establishment of stable links between distant antiparallel actin protofilaments after a local myosin II activation may initiate the repair of the disrupted area. We show that it is possible to define conditions in which the calculated number of myosin II minifilaments bound to actin protofilaments is consistent with the estimated number of myosin II minifilaments present in the red blood cells. A clear restoration effect can be observed when more than 50% of the spectrin polymers of a defined area are disrupted. It corresponds to a significant increase in the spectrin density in the protein free region of the membrane. This may be involved in a more complex repair process of the red blood cell membrane, which includes the vesiculation of the bilayer and the compaction of the disassembled spectrin network.

INTRODUCTION

The deformability of red blood cells (RBCs) allows these cells to pass through capillaries that are about half their diameter (7 μm) without any damage (Gratzer, 1981; Branton et al., 1981; Shohet and Mohandas, 1988). The plasticity of RBCs relies on a specific cytoskeleton that is closely associated with the inner face of the membrane (Bennett and Branton, 1977; Marchesi, 1985; Bennett, 1985). It consists of a hexagonal network of spectrin tetramers interconnected at their ends by short (~600 Å) actin protofilaments made of 13 protomers. These actin protofilaments associated with rodlike tropomyosin (Fowler, 1996) can bind several spectrin tetramers to form a multiprotein network that is anchored to the membrane and strengthened by ankyrin (Bennett and Stenbuck, 1980) and protein-4.1 (Pekrun et al., 1989; Tchernia et al., 1981; Waugh, 1983).

RBCs contain ~240,000 spectrin molecules (Agre et al., 1985), each of which consisting of two antiparallel coiled α- and β-chains associated side by side (Speicher et al., 1992; Yoshino and Minari, 1991). A further head-to-head association of these spectrin dimers allows the formation of tetramers of length 820-1920 Å (Elgsaeter et al., 1986; Bloch and Pumplin, 1992), which in turn constitute a dynamic network able to adapt to the biophysical environment of the cell. This plasticity was demonstrated on normal RBCs that were deformed after a prolonged micropipette aspiration and on RBCs taken from patients with sickle cell anemia (Speicher et al., 1992; Liu et al., 1996). The shape adaptation of RBCs is most often accomplished by the dissociation of the spectrin network followed by its reassociation in a new configuration (Liu et al., 1993, 1996; Hansen et al., 1997).

During aging, RBC functions can be impaired by either chemical (free radical damage) or mechanical shear stresses inducing alterations of certain cellular characteristics, such as disruption of spectrin tetramers, band-3 hydrolysis, aggregation of intrinsic membrane proteins, appearance of protein-depleted gaps in the RBC membrane skeleton, and formation of Heinz bodies (Leverett et al., 1972; Waugh and Low, 1985; Waugh et al., 1986; Solar et al., 1990; Fukushima and Kon, 1990). These features act as tags of the older RBCs, which are then detected and eliminated by the reticuloendothelial system (Schluter and Drenckhahn, 1986).

RBCs possess a small number of myosin II molecules (Colin and Schrier, 1991), although they do not show any apparent contractility. Myosin II has been characterized in neonatal and adult human as well as bovine erythrocytes (Higashihara et al 1989; Wong et al., 1985; Fowler et al., 1985; Schluter and Drenckhahn, 1986; Matovcick et al., 1986; Higashihara et al., 1989). Human RBC myosin II appears to be structurally similar to other nonmuscle myosin IIs. It consists of two heavy chains (200 kDa) and two pairs of regulatory and structural light chains (Wong et al., 1985; Tan et al., 1992; Trybus, 1991). The presence in RBCs of calmodulin (Foder and Scharff, 1981), caldesmon (Der Terrossian et al., 1994), tropomyosin (Fowler, 1996; Fowler and Bennett, 1984), and myosin light chain kinase (Knipper et al., 1995) has been reported. These results taken together

Received for publication 12 March 1998 and in final form 22 October 1998.

Address reprint requests to Dr. C. Cibert, Laboratoire de Biologie du Développement, Institut Jacques Monod, UMR 7592, CNRS, Universités Paris VI et Paris VII, 2, place Jussieu, F-75005 Paris. Tel.: 33-1-44278161; Fax: 33-1-44275265; E-mail: cibert@ijm.jussieu.fr.

0006-3495/99/03/1153/13 $2.00

raise the possibility of the presence of a Ca^{2+}-dependent actomyosin II ATPase activity in the RBC.

No clear function for this putative ATPase has been assigned (Schrier et al., 1981; Matovcick et al., 1986). It has been proposed that the presence of such a small quantity of myosin II may simply be the consequence of the incomplete removal of myosin II during the expulsion of the nuclei and associated structures from the reticulocytes. However, there is evidence that myosin may participate in the regulation of the RBC shape (Fowler, 1986), involving a rapid kinetic process with regard to the displacement of RBCs in the blood flux.

In this theoretical study, we propose a contribution of the actomyosin II complexes in the repair of a local disruption of spectrin network. A mathematical model of the membrane skeleton (Saxton, 1992) was used to analyze this function. The involvement of myosin II minifilaments in a general repair process of the RBC bilayer-skeleton unit is proposed.

MATERIALS AND METHODS

Computer and software

The main software was written specifically for this study, using the C-interpreter of Visilog 4.1.1 image analysis software (Noesis, Orsay, France) running on a SiliconGraphic Indigo (4000 entry) workstation (Mountain View, California, USA).

Theoretical skeleton

We have constructed a hexagonal matrix according to the method of Saxton (1992), which corresponds to the theoretical spectrin network. The hexagonal unit is a six-armed star consisting of spectrin tetramers interconnected by actin protofilaments and associated proteins (Fowler, 1996). Junction complexes were defined as the apices of the hexagons and include actin protofilaments. In our calculations, the length of the spectrin tetramers in the native matrix (820 Å) was taken as the length unit (LU) and was equal to ~16.5 pixels (Fig. 1, *upper left image*). The matrix used consisted of 494 junction complexes and 1210 spectrin tetramers.

Random disruption of spectrin tetramers and calculation of the matrix equilibrium (Fig. 1)

A random image with an area equal to the number of spectrin tetramers was generated (the rank of each pixel corresponded to the rank of each spectrin tetramer in the matrix). The gray-level histogram of this image was Gaussian (dynamic range 1–254). To define the random disruptions of the spectrin tetramers, this random image was thresholded to obtain a binary image with an area corresponding to the number of altered spectrin tetramers.

Increasing percentages of random disruptions of the spectrin tetramers (from 5% to 70% with a 5% increment) were generated on square windows (~0.7 μm^2) within the theoretical skeleton. A buffer zone in which the percentage of random disruptions was held constant at 5% was defined outside this window (Hansen et al., 1997). The entropic spring approximation was then used to calculate the matrix conformation after each random disruption (Saxton, 1992). When the equilibrium of the central junction complex of each of the hexagonal units was calculated in the presence of actomyosin II complexes, only the extended complexes limited their relative motion. The maximum extension for actomyosin II complexes was equal to the distance between the two junction complexes. When only one actomyosin II was extended, the displacement of the central junction complex was restricted to the circle centered on the linked neighbor. When two or more were extended, the two most extended were considered to be the limiting factors. We supposed 1) that the compression modulus for myosin II minifilaments is null and 2) that the actomyosin II association is stable (latch state; Trybus, 1991). During the calculation, the formation of actomyosin II complexes imposed the orientations of the actin protofilaments involved.

The disrupted spectrin tetramers were considered to be unable to reconstruct other spectrin polymers as previously described (Liu et al., 1993) and/or calculated (Hansen et al., 1997).

Weight of activated actin protofilaments (Fig. 1)

The weight defines the probability that each of the actin protofilaments is involved in an actomyosin II complex within the impaired area. It was calculated as follows. For each hexagonal unit, the Euclidean intervals between the central junction complex and its six neighbors were calculated. We assumed that the maximum of these intervals could be 1) lower than LU, 2) between 1 and 2 LU, and 3) larger than 2 LU. The corresponding weight of the central junction complex was then 1) equal to 0, 2) calculated according to a linear scale from 0 to 255, or 3) equal to 255, respectively. After this first calculation, the weight of the central junction complex of each of the hexagonal units was calculated as the mean of the seven associated ones (the weight of the central junction complex of a given unit was multiplied by p ($p = 100$)). The convergence was obtained with an iterative calculation of these mean values. After convergence, the "activated" junction complexes were selected by thresholding. We have arbitrarily assumed that the percentage of spectrin disruption in a native membrane is lower than 15%. The maximum weight that we calculated for this percentage of random disruption was equal to 115.75. This value was chosen as the lower limit above which the junction complexes may be "activated" and involved in the network restoration.

Myosin II minifilament architecture

According to Sinard et al. (1989) and Tan et al. (1992), myosin II can form tightly elastic bipolar minifilaments resulting from the association of either 4 or 16 myosin II molecules (Fig. 2, *A* and *B*), which we define as MII_4 and MII_{16}, respectively. We assumed that the lengths of MII_4 and MII_{16} varied from −10% to +2%, i.e., between 2430–2700 Å and 2970–3300 Å, respectively. These variations were converted as an abitrary 52° bending of the minifilaments.

Orientation, free rotation, and effective length of the actin protofilaments (Fig. 2 *C*)

Actin protofilaments were arbitrarily oriented in 16 directions of the membrane plane. The rotation of the actin protofilaments depends on the number of spectrin tetramers linked to each junction complex. The freedom (f) of the actin protofilaments was taken as $f = (6 - s) * q$, where s is the number of intact spectrin tetramers and q is the angular rotation increment (30°). This corresponds to the free rotation of the protofilament on both sides of its original orientation. As an example in Fig. 2 *C*, the freedom of the A0 and Ai protofilaments equals 60° and 90°, respectively. A_{min} and A_{max} defined the intervals between the junction complexes and the beginning or the end of the effective length of the actin protofilaments, respectively (*dashed circle*); this effective length (A_{min}, A_{max}) defines the segment on which myosin heads may interact with one actin protofilament.

Actomyosin II formation (Fig. 2 *C*)

To calculate the location of the MII minifilaments on the actin protofilament of each of the activated junction complexes, we determined the activated actin protofilaments located in a crown around the junction

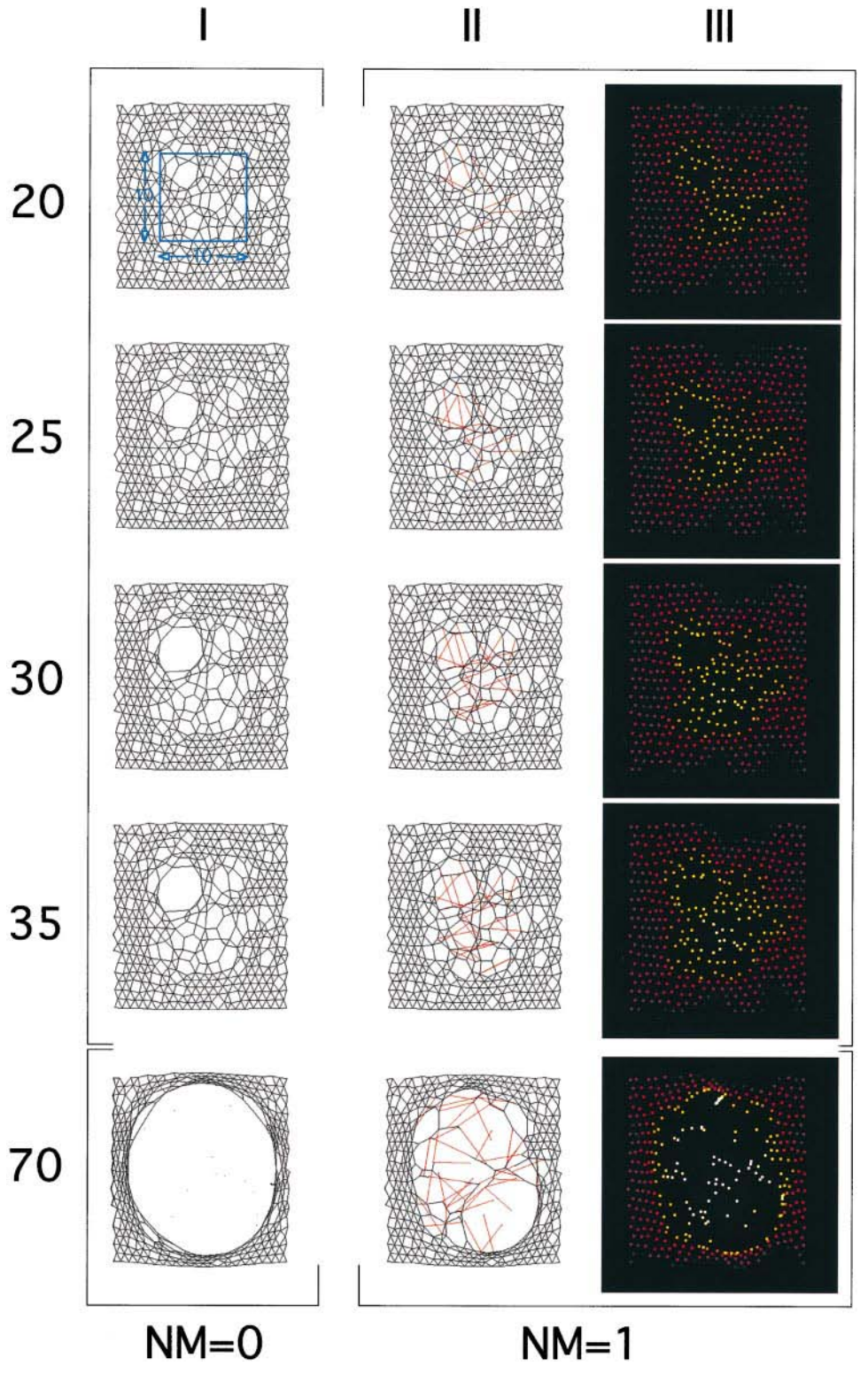

FIGURE 1 Matrix equilibrium without (NM = 0, first column) or with (NM = 1, *second column*) myosin II and weight of the junction complexes (*third column*). The percentage of spectrin disruption inside the blue window (*upper left image*) is indicated on the left of the figure and was held constant at 5% outside. In the first two columns the spectrin meshwork is black. In the second column, actomyosin II complexes are indicated in red. The weight of the junction complex is calculated in the presence of myosin II (NM = 1, A_{min} = 0 and A_{max} = 60) and expressed on a gray scale ranging between 0 and 255. NM is the maximum number of MII minifilaments that may be linked to each actin protofilament.

complex. The internal and the external diameters of the crown corresponded to the sum of the MII minifilament length and twice either the minimum (A_{min}) or the maximum (A_{max}) of the actin protofilament, respectively. Only the actin protofilaments showing an orientation compatible with the one of the actin protofilament associated with a considered junction complex were retained. The number of myosin II heads retained on each of the actin protofilaments was taken as equal to (or lower than) the theoretical value defined at the beginning of the calculation (NM, where NM $\in$ [0, 20]). It involved the actin protofilaments, which were classified as a function of their decreasing weight.

Density of junction complexes (Fig. 3)

The apparent density of the junction complexes was calculated as the superposition of a disc representing their individual area of influence (AOI)

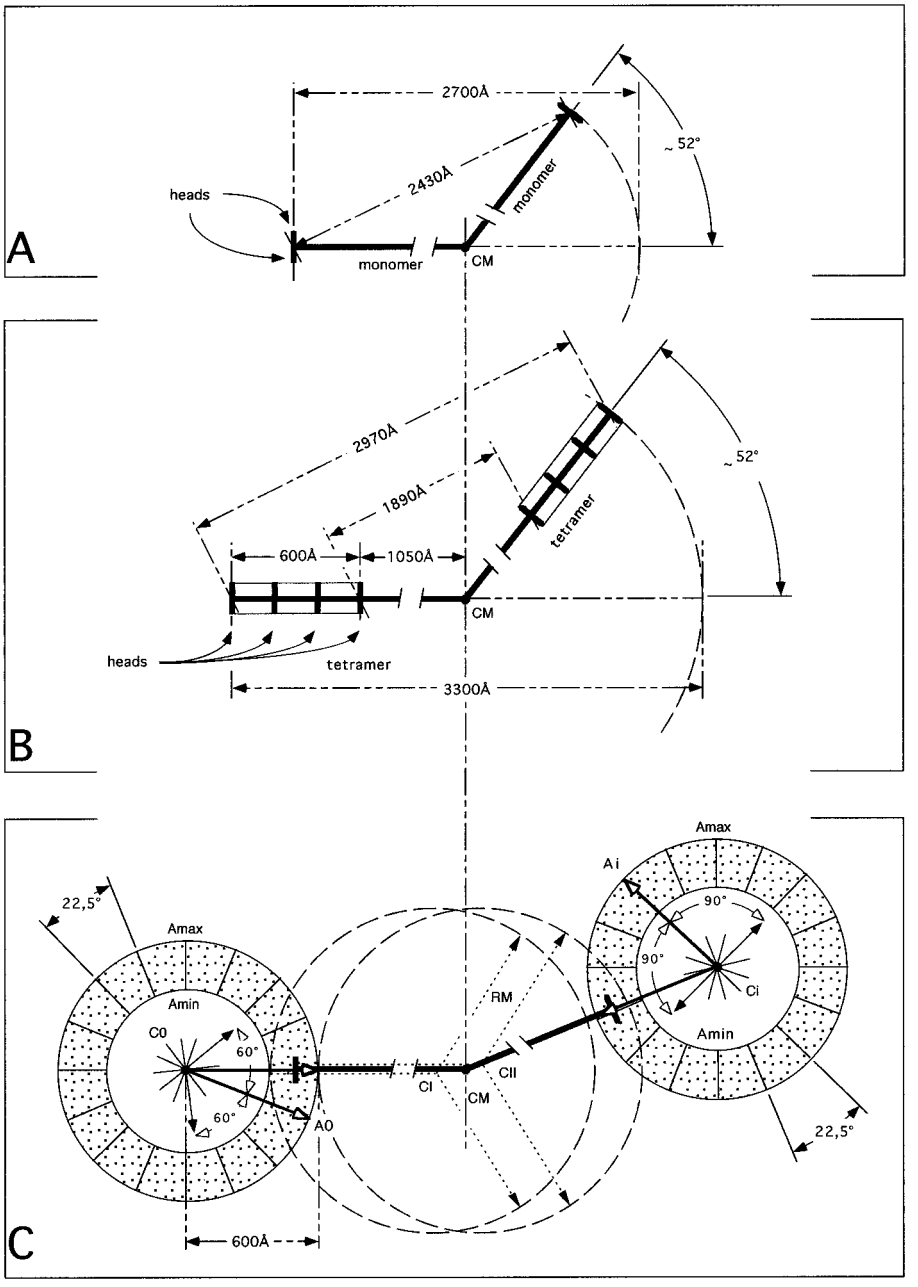

FIGURE 2 Structure of the MII_4 (*A*) and MII_{16} (*B*). MII_4 and MII_{16} were considered to be slightly elastic tetramers ~2700 Å and 3300 Å long, respectively. Their shortening (−10%) was expressed in terms of bending (~52°). (*C*) Actomyosin-II association. Actin protofilaments (600 Å long) were randomly oriented in 16 directions of the plane (22.5° increment). This orientation was fixed as long as the spectrin network remained intact. The freedom of actin protofilaments may increase with the percentage of spectrin tetramers disrupted. The effective length of protofilaments is equal to $A_{min} - A_{max}$. C0 and CI correspond to the ranks of the two junction complexes of the Saxton's matrix. A0 and Ai are the actin protofilaments associated with C0 and CI, respectively. CM is the bending center of MII_4, and CI and CII correspond to the positions of these centers if the heads of MII_4 shift between A_{min} and A_{max} on A0. RM is the length of the myosin II dimer. The interaction between actin and myosin II is possible if the antiparallelism between the actin protofilaments and the MII minifilaments is respected.

with an associated gray level equal to 5. The centers of the AOIs corresponded to the junction complexes themselves, and their diameters equaled 0.5 LU. After convergence, we expressed the relative density of the junction complexes as the local sum of their individual AOIs.

RESULTS

Conditions for MII_4 location

As shown in Figs. 1 and 3, a large gap was observed inside a ~0.7-μm^2 window representative of the skeleton when 70% of the spectrin tetramers were disrupted randomly in the absence of the formation of actomyosin II complexes.

We constructed a spectrin network restoration model according to which all of the activated junction complexes with a weight higher than 115.75 can participate in the repair. To render this model plausible, the number of MII_4 involved in the local restoration of the skeleton inside a given window had to fit with their corresponding local density (~3.6–9.2 $MII_4/\mu m^2$; see Discussion). To decrease the stringency of the theoretical low density, we arbitrarily considered that the recruitment of the MII_4 may occur in the six or eight equivalent windows surrounding the disrupted one (Fig. 4). At first it was assumed that only one myosin II head could be linked to each activated actin protofilament (NM = 1). Three topological characteristics were then considered: 1) the effective length of the actin protofilaments (A_{min}, A_{max}), 2) the relative orientation between actin protofilaments and MII_4, and 3) the degree of freedom of

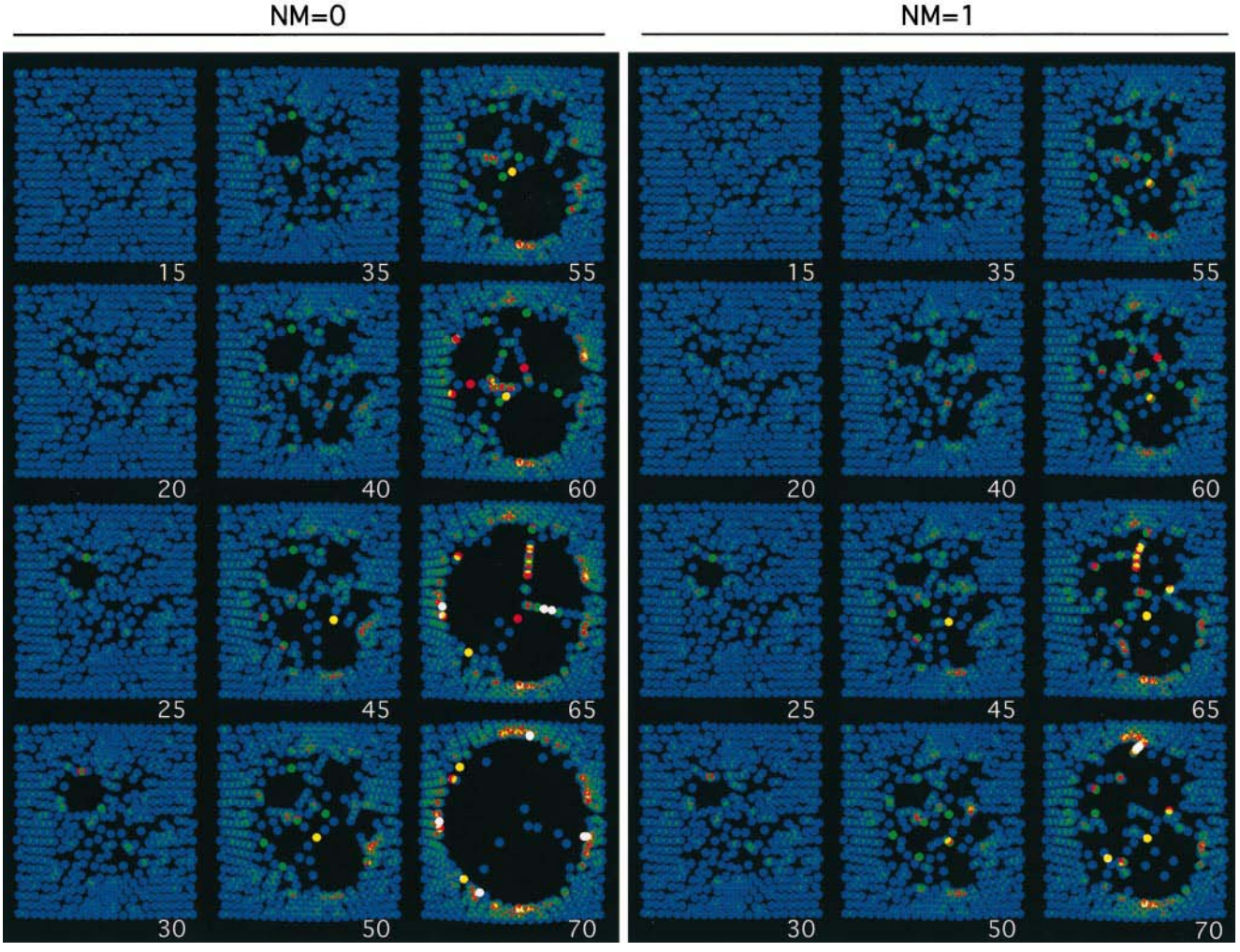

FIGURE 3 Density of the junction complexes. The area of influence (AOI) of each of the junction complexes is shown in blue. The superposition of these AOI defines the local density of the junction complexes. Green, red, yellow, and white correspond to the superposition of two, three, four, and more than four AOIs, respectively. The percentage of spectrin tetramers disrupted is indicated in the lower right corner of each of the images. The left and right panels correspond to the density of the Saxton's matrix when NM = 0 or NM = 1, respectively. In these calculations (A_{min}, A_{max}) = (0, 60).

actin protofilaments. After the incidences of these parameters were measured, the effects of the NM variations on the equilibrium of the matrix were quantified.

Effective length for actin protofilaments

To test the incidence of the effective actin protofilament length, we assumed that they are attached by their barbed ends to a junction complex and can move freely in a 2π disc around it. Three effective pairs of values were then considered for (A_{min}, A_{max}): (0, 0), (0, 60), and (60, 60), corresponding to the junction complex itself, the entire protofilament length, and the protofilament pointed end, respectively (Shen et al., 1986; Fowler, 1996). The calculation was carried out on the impaired 0.7-μm^2 area in which 15–35% of the spectrin tetramers were disrupted, taking into account the effect of MII_4 on the geometry of the matrix (Fig. 5).

With no constraint other than the MII_4 length itself (f = 180°) (Fig. 5, *row* − −), the total numbers of MII_4 that were calculated on the matrix under the three sets of conditions were equal to 42, 43, and 37, respectively. Thus the effective actin protofilament length did not seem to be a limiting factor for actomyosin II complex formation. Moreover, the topology of the MII_4 distribution was quasiequivalent under the three sets of conditions, even if the higher number of MII_4 potentially induced a locally more condensed actomyosin II pattern.

These numbers of MII_4 (~40) were always higher than 10 times the theoretical local density of molecules beneath the membrane. This high number of MII_4 would then have to be recruited from more than six or eight equivalent windows (7 * 3.6 ≈ 25, 9 * 3.6 ≈ 32), which is incompatible with the isotropic recruitment model we postulated and the lower density of the minifilaments.

A similar set of calculations was made with (A_{min}, A_{max}) = (0, 38.4), where A_{max} corresponds to the shortest length assigned to an actin protofilament in RBCs: 384 Å

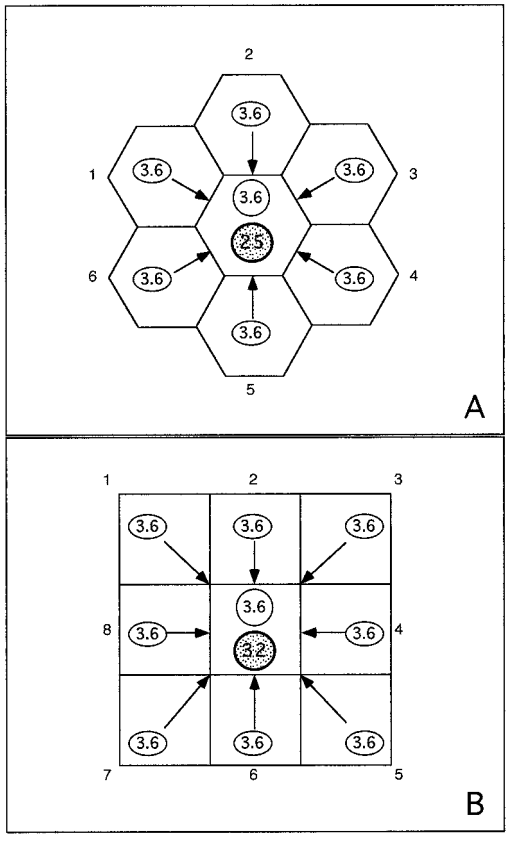

FIGURE 4 Recruitment of the MII minifilaments over the membrane. Diagram of the MII minifilament recruitment, considering either the 6-neighborhood (*hexagonal grid*) (*A*) or the 8-neighborhood (*rectangular grid*) (*B*) organizations of the membrane skeleton. The values correspond to the recruitment of the MII_4 with a density equal to $3.6/\mu m^2$ (see text).

(Shen et al., 1986). The results were similar to those that we observed when (A_{min}, A_{max}) = (0, 60).

Orientation and freedom of actin protofilaments

The actin protofilaments were considered to be able to move in a 2π steradian solid angle, and their orientations were defined as the projection in the membrane plane of 16 possible orientations (Fig. 2 *C*), the perpendicular position being omitted. The calculation showed that no actomyosin II complex could be formed when the fixed actin protofilament orientations were considered (data not shown). Thus it is impossible for two activated junction complexes to include two antiparallel actin protofilaments at a distance compatible with MII_4 lengths when the orientation of protofilaments is randomly defined and fixed over the matrix. The orientation of actin protofilaments appeared to be the principal limiting factor for the formation of actomyosin II complexes.

When the degree of freedom of the actin protofilaments is correlated with the degree of disruption of the spectrin tetramers, the effective length becomes a limiting factor. Both actin protofilament freedom and effective length influenced the number and the spatial distribution of MII_4 (Fig. 5, *row* ++). When 35% of the spectrin tetramers were disrupted, the most favorable results were obtained with the active actin protofilament length equal to 600 Å (A_{min}, A_{max}) = (0, 60). In this case, 22 possible links could be formed. This number was compatible with biological data and with the limits considered for our model (i.e., lower myosin density and hexagonal partition of the peripheral cytoplasm). As shown in Table 1 *A*, for NM = 1 and when 40% of the spectrin tetramers were locally disrupted, the total number of calculated actomyosin II complexes was equal to 33. This value corresponds to a rectangular partition of the peripheral cytoplasm and is still compatible with the theoretical limits (Fig. 4).

In the different conditions set above, the network restoration of ~0.6% (1 μm^2) of the total membrane area might involve between ~4% (for 35% disruption) and ~6% (for 40% disruption) of the peripheral cytoplasmic volume of the blood cell.

Effect of the number of actomyosin II complexes on the topology of the network restoration

The effects of the number of MII_4 associated with each actin protofilament were calculated. We assumed that the actin protofilament effective length was equal to 600 Å (A_{min}, A_{max}) = (0, 60) and that their freedom increased as a function of the number of disrupted spectrin tetramers.

We have calculated the equilibrium of the matrix when NM equaled 1, 2, 3, 4, 5, or 6 (Table 1). We have compared the patterns of the spectrin skeleton matrices obtained after a disruption of either 35% or 70% of the spectrin tetramer (Fig. 6). When 70% of the spectrin tetramers are disrupted, 1) the total number of linked actin protofilaments is constant (~90) whatever the value of NM, 2) 5 is the maximum number of MII_4 that can be calculated, and 3) only 10 actin protofilaments support either 3 or more MII_4. This shows that raising NM from 3 to 5 neither increased the number of linked actin protofilaments nor changed the geometries of spectrin tetramers or junction complexes significantly (Fig. 6).

Network restoration and densities of junction complexes

We have measured the superposition of the junction complexes' AOIs and observed that they increase with the percentage of spectrin disruption inside the window (Table 2, *A* and *B*). However, the distribution of the AOIs in the matrix plane (Fig. 3) showed that the gap is balanced by the displacement of all of the junction complexes in the membrane plane. This reflects the fact that the local disruption of spectrin tetramers is associated with an increase in the AOI density not only at the border of the gap, but also within a large crown around it (except for the highest disruption, ≥65% of spectrin disruption). The data shown in Table 2

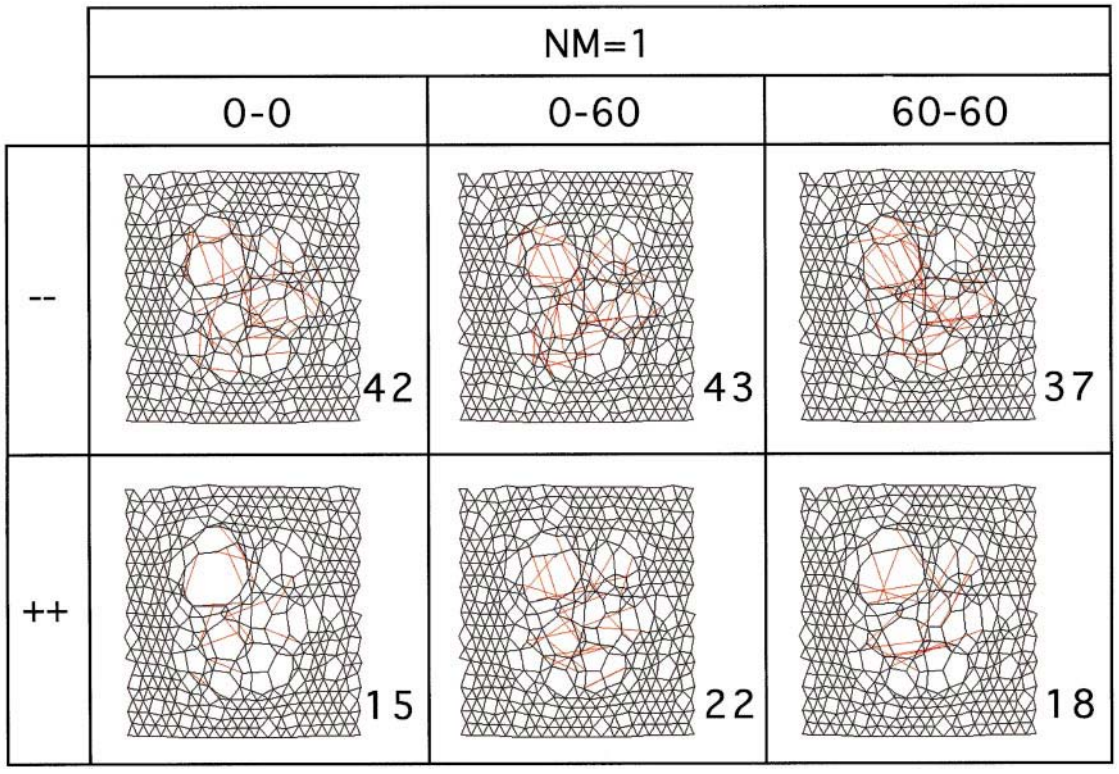

FIGURE 5 Effect of the actin protofilament effective length and orientation (NM = 1). The percentage of spectrin disruption equals 35%. The effective length of the actin protofilaments was restricted to the junction complex (0–0), equal to their whole length (0–60) or restricted to their tip (60–60). *Row* −−: The calculation of actomyosin II complexes was realized only when the interval between two activated actin protofilaments was taken into account. *Row* ++: The same calculation was realized when the orientations of the actin protofilaments were randomly fixed and increased as a function of the local spectrin disruption. The number of actomyosin II complexes was calculated step by step between 20% and 35% of local random spectrin disruption and is indicated in the lower right corner of the image. The skeleton and the actomyosin II complexes are colored in black and red, respectively.

strengthen this calculation. In the presence of actomyosin II complexes, the number of AOIs superposed once or not at all, calculated as a function of the increasing disruption percentage (Table 2 *B*), is never <70%, whereas it can go down to 59% in the absence of actomyosin II complexes.

The comparison of the AOI density patterns obtained in the absence or presence of MII_4 (Fig. 3) shows that 1) the actomyosin II complexes are able to decrease slightly the extension of the gap after an important disruption of the spectrin tetramers (between 35% and 70%) and 2) the main effect of actomyosin II complexes is to maintain some junction complexes inside the area when the major part of the skeleton is disrupted.

There is no difference in the matrix topologies or AOI density when NM varies from 3 to 5. Therefore, we assumed that the maximum effect is obtained when NM = 3 (Fig. 6). But because NM = 1 is sufficient to promote an equivalent restoration, and because under this condition the number of actomyosin II complexes is compatible with the lower local density of MII_4 in the peripheral cytoplasm (whatever the percentage of the disrupted spectrin polymers), we propose that NM = 1 is the condition most likely to ensure an efficient restoration of the spectrin network in a large gap.

Rank and bending of the myosin polymers

The effects of the rank of the myosin II polymers (MII_4 and MII_{16}; Fig. 2, *A* and *B*) were calculated. The effects of the two types of MII minifilaments on both the number of actomyosin II complexes and the network restoration efficiency were almost identical.

One of the most important results is that the bending of MII minifilaments was not absolutely necessary for the network restoration efficiency, because more than 80% of the actomyosin II complexes are formed even if the MII minifilaments are not bended, as compared to 100% when they are bended.

DISCUSSION

In RBCs shear stress or oxidative damage due to free radicals induce the local disruption of the spectrin tetramer network and a subsequent hemolysis (Jarolim et al., 1990; Daniels et al., 1983; Waugh and Low, 1985; Waugh et al., 1986). In the present theoretical approach, we propose that actomyosin II complexes are involved in the repair of the erythrocyte spectrin skeleton via a network restoration mechanism. Our model involves a stable linkage of actin

TABLE 1 Effect of NM variation

	Number of added MII-minifilaments					
% Cut	NM = 1	NM = 2	NM = 3	NM = 4	NM = 5	NM = 6
A						
15	0	0	0	0	0	0
20	6	13	14	14	14	14
25	4	8	11	11	11	11
30	7	9	12	12	12	12
35	5	6	6	6	6	6
40	11	15	19	21	22	22
45	2	2	1	1	1	1
50	1	0	0	0	0	0
55	5	3	5	5	5	5
60	1	1	0	0	0	0
65	1	1	0	0	0	0
70	1	1	0	0	0	0
Sum	44	59	68	70	71	71
Linked actins	88	89	89	90	91	91
n	Number of linked junctional complexes					
B						
0	402	405	405	404	403	403
1	92	60	52	52	53	53
2		29	27	28	28	28
3			10	8	8	8
4				2	1	1
5					1	1
6						0

(A) Number of added MII_4 as a function of NM and the percentage of spectrin tetramer disruption. The maximum number of actomyosin II complex is obtained if NM = 3. When NM = 1, the sum of the calculated actomyosin II complexes between 20% and 40% of spectrin tetramer disruption equals 33. (B) Number of *n* times linked junction complexes in function of NM. When NM = 3, 4, and 5 we observe only a modification of the distribution of 3, 4, and 5 times linked actin protofilaments. In these calculations $(A_{min}, A_{max}) = (0, 60)$.

protofilaments by bipolar MII minifilaments around the damaged area of the network, which can then facilitate the reorganization of the whole cytoskeletal ultrastructure. The topological consequences and the efficiency of this model were studied with regard to the physiological activity of the "bilayer-skeleton unit."

Different mathematical models have been proposed to calculate the RBC spectrin network architecture as a function of different biophysical parameters (Kozlov et al., 1990; Saxton, 1992, 1995; Boal, 1994; Hansen et al., 1997). The actual positions of the junction complexes in the hexagonal matrix move around a mean "3D" location as a function of time and dynamic conformation of spectrin tetramers (the theoretical thickness of the skeleton is ~160 Å; Boal, 1994). It has been proposed that spectrin tetramers may act as entropic springs (Saxton, 1992). Although this simple model does not take into account all of the parameters involved in the skeleton topology, it allows one to calculate the consequences of local disruptions of spectrin tetramers.

It was demonstrated that small protein-free areas (with a critical radius of ~1000 Å) are submitted to an "auto-opening" and "auto-closing" equilibrium (Kozlov et al., 1990). This equilibrium depends on 1) the shape of the membrane (planar, cylindrical, or spherical) and on 2) the energy associated with the local extension of the cytoskeleton. This could explain the dynamics of the RBC skeleton during spicule formation. The radii of the largest gaps remained inferior to the critical radius for a percentage of disrupted spectrin tetramers below 15%. The repair was not necessary for a disruption of spectrin tetramers lower than this limit. The maximum length of the remaining spectrin tetramers was subsequently determined for each step of the calculation between 15% and 70% of local spectrin disruption, with or without MII_4 addition. The length values ranged between 1.37 and 2.05 LU and were never higher than the spectrin tetramer maximum length (~2.5 LU) (Bloch and Pumplin, 1992), rendering the mechanical tearing of gaps very improbable (data not shown).

Some arguments suggest a functional role for RBC myosin II. It is thought that MII minifilaments are involved in the remodeling of the RBC shape (Fowler, 1986; Colin and Schrier, 1991). The amounts of myosin II in different fractions of RBCs were measured under conditions that favor the interaction between actin and myosin (Matovcick et al., 1986), especially in skeleton preparations and inside-out vesicles. Myosin II is retained on IOVs that are enriched in integral membrane proteins (Steck and Kant, 1974; Bennett and Branton, 1977). Moreover, the disruption of the skeletal network induces the specific adsorption of myosin II to the membrane bilayer and/or to membrane proteins (protein-4.1, for example, is able to link myosin II; Racusen and Pasternack, 1990).

The Ca^{2+} activation of the actomyosin II machinery in RBCs seems to be similar to that in smooth muscle cells (Trybus, 1991; Tan et al., 1992) or other biological systems (Chrzanowska-Wodnicka and Burridge, 1996). In RBCs, the internal calcium concentration $[Ca^{2+}]_i$ depends on the equilibrium between passive influx and active efflux through a membrane Ca^{2+}-ATPase activity (Larsen et al., 1981; Graf and Penniston, 1981; Niggli et al., 1981; Kosk-Kosicka and Bzdega, 1988; Adamo et al., 1990; Sackett and Kosk-Kosicka, 1996). During a shear stress, the passive influx increases by up to one order of magnitude (Larsen et al., 1981; Johnson and Tang, 1992; Kodicek et al., 1990). When this influx increase occurs in the peripheral cytoplasm around the area of damaged cytoskeleton, the local $[Ca^{2+}]_i$ may rise enough to allow a local and rapid formation of actomyosin II complexes (Foder and Scharff, 1981; Ogawa and Tanokura, 1984; Milos et al., 1986; Gardner and Bennett, 1986; Ikebe and Reardon, 1990; Tanaka et al., 1991; Tan et al., 1992; Marston and Redwood, 1993; Der Terrossian et al., 1994). The local protein density may also be involved in the modulation of $[Ca^{2+}]_i$. Because the local effect of spectrin tetramer disruption is to induce a protein-free area (Fig. 1), it may be postulated that the calcium pulse is amplified because of the local decrease in proteins that can chelate Ca^{2+}, as spectrin does (Lundberg et al., 1992).

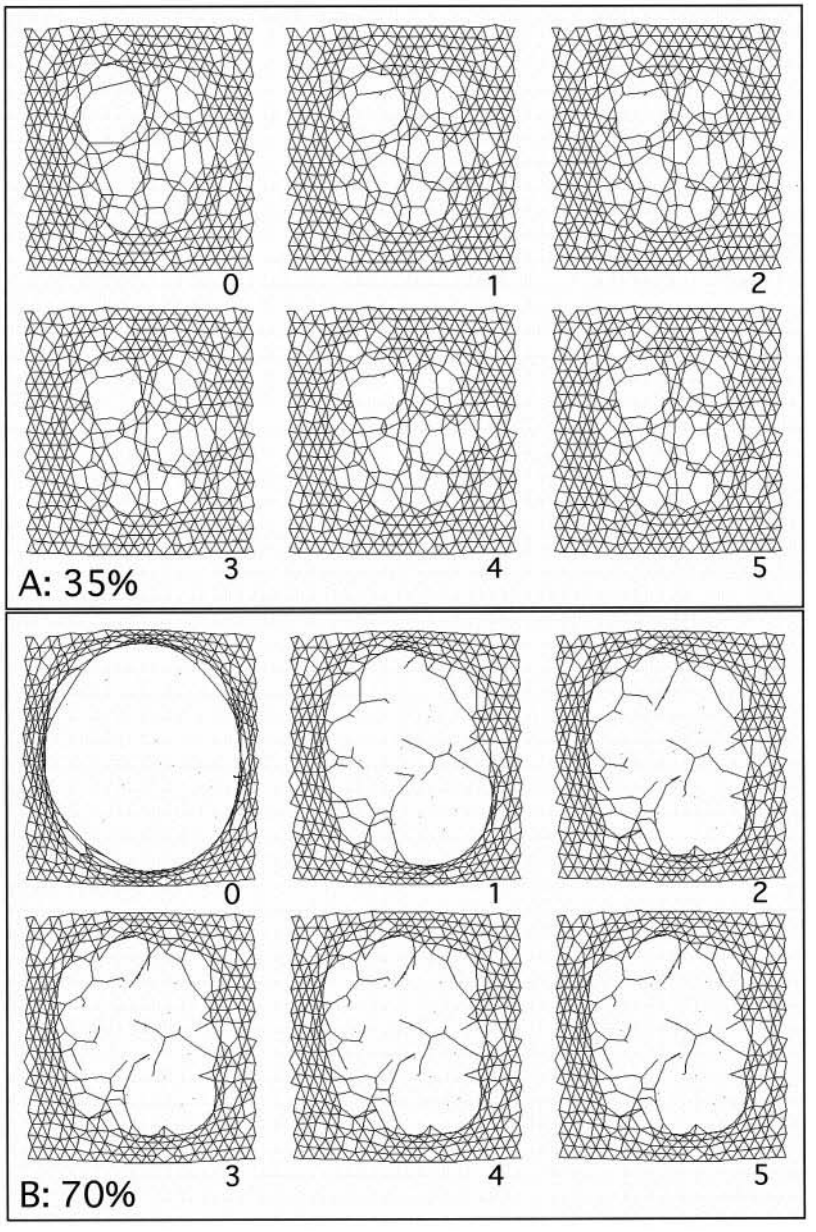

FIGURE 6 Effect of the MII_4 number (NM) on network restoration efficiency. Spectrin network equilibrium convergence after either 35% (*A*) or 70% (*B*) of random spectrin tetramer disruption in the presence of different amounts of actomyosin II complexes when (A_{min}, A_{max}) = (0, 60). For each image the value of NM is indicated in the lower right corner. The main effect on the network restoration is that the junction complexes are maintained within the gap, even when spectrin disruption is severe. From these images, it appears that when NM ranges from 3 to 5, the same repair effect is observed.

The number and the location of myosin II molecules inside the RBCs are two basic parameters involved in our model. The number of the myosin II molecules was estimated to be between 2400 and 6000 per cell (Wong et al., 1985; Fowler et al., 1985). Consequently, the theoretical number of MII_4 ranges from 600 to 1500. Immunofluorescence observations using antibodies directed against myosin II revealed that myosin is mainly located in the ~1 μm-thick peripheral cytoplasm of the RBC (data not shown). Thus the density of myosin II in RBCs must range between 3.6 and 9.2 $MII_4/\mu m^2$ of membrane, considering that the red cell membrane area is ~163 μm^2 (Albritton, 1952).

To limit the number of MII_4 that may be involved in the local network restoration and to avoid a large decrease of MII_4 all over the membrane, we have defined hexagonal or rectangular virtual organizations of the peripheral cytoplasm (Fig. 4). We postulated that the myosin II molecules could only be recruited from the six or eight equivalent areas surrounding the disrupted region. At the lowest myosin II density, the maximum number of MII_4 that must be involved in the restoration of a 1-μm^2 window ranges from ~25 ((6 + 1) * 3.6) to ~32 ((8 + 1) * 3.6).

To respect this limit when the restoration occurs in an area in which over 15% of the spectrin tetramers have been disrupted, several sterical parameters were taken into account: 1) the effective length and 2) the free rotation of the actin protofilaments; 3) the folding and 4) the number of MII_4 that may be linked to one actin protofilament; and 5) the local activation (weight) of the junction complexes around the impaired area. When 1) the effective length of actin protofilaments equals 600 Å, 2) their orientation is randomly fixed, and 3) their freedom increases as a function

TABLE 2 Superposition of the junction complex AOIs

% Cut	15	20	25	30	35	40	45	50	55	60	65	70
Superposition	%	%	%	%	%	%	%	%	%	%	%	%
A												
0	99.93	99.73	98.98	97.71	98.95	97.36	91.86	91.17	89.74	83.31	73.48	58.99
1	0.07	0.27	1.02	2.29	1.05	2.64	6.48	6.97	8.17	13.30	16.16	15.27
2							1.66	1.86	1.98	3.08	5.88	6.47
3									0.10	0.30	2.71	3.14
4										0.01	1.19	2.61
5											0.37	2.40
6											0.20	2.11
7											0.01	1.71
8												1.42
9												1.27
10												1.19
11												1.15
12												0.94
13												0.68
14												0.36
15												0.22
16												0.08
B												
0	99.93	99.73	98.92	97.93	98.50	96.95	90.83	91.16	92.23	90.12	78.96	72.67
1	0.07	0.27	1.08	2.07	1.50	3.05	7.11	7.34	6.71	8.76	15.15	14.58
2							2.04	1.48	1.06	1.12	5.18	6.55
3							0.02	0.02			0.65	2.06
4											0.05	1.33
5												0.65
6												0.49
7												0.35
8												0.16
9												0.02
10												
11												
12												
13												
14												
15												
16												

(A) and (B) give the percentages of the superposition of these AOIs as a function of the percentage of random disruption of the spectrin polymers (ranging from 15% to 70%) in the absence and presence of MII_4, respectively.

of the local disruption of the spectrin meshwork, the calculated number of actomyosin II complexes for NM = 1 is compatible with the lowest limits that we have defined.

The maximum restoration was obtained for NM = 3 (Fig. 6). This is in agreement with the theoretical density of myosin heads per actin protofilament (3.3 myosin heads/600 Å actin protofilament; Van Buren et al., 1995). However, the same local topological effects were obtained whenever NM was equal to either 1 or 3; NM = 1 is sufficient to ensure the restoration of the network (Fig. 6). This value is compatible with the low density of MII minifilaments in proximity to the locally disassembled spectrin network.

To estimate the biological efficiency of this restoration, we took into account the "corrals of actomyosin II complexes" that we obtained. According to Kozlov et al. (1990) and Saxton (1995), corrals of spectrin tetramers correspond to small areas where cytoplasmic molecules can interact directly with the bilayer. Figs. 1 and 5 show that actomyosin II complexes do not reconstruct new corrals of spectrin over all of the disrupted area because they are longer than the native spectrin tetramers and do not associate with the bilayer the same way as spectrin does.

The most important geometrical effect of the passive network restoration that we have observed is the increase in the density of junction complexes inside the impaired area. As shown in Fig. 3, this effect is observable when the percentage of spectrin tetramer disruption reaches 30% and above.

The passive restoration efficiency of the spectrin network that we have calculated seems to be limited. But it may

induce the local dynamic reorganization of the spectrin tetramers inside the damaged area (Liu et al., 1993; Hansen et al., 1997).

The involvement of MII minifilaments in a dynamic repair process has already been observed in cultures of epithelial cells and described as a "purse-string" mechanism; the actomyosin II complexes form a ring around the wound that must be sealed (Bement et al. 1993). In this case, myosin II is involved in the repair of a wound the diameter of which may be over 30 μm (area $> 700\ \mu m^2$). In our case, the area of the impaired area is $\sim 1\ \mu m^2$, and the actomyosin II network that we have calculated tends to link the opposite edges of the wound, the diameter of which is near the length of the actomyosin II complexes themselves. The dynamic process that we propose corresponds to the compacting of the disassembled spectrin network area associated with lipid bilayer vesiculation.

The relationship between the dynamic behaviors of the lipidic bilayer and the erythrocyte membrane skeleton during stress is well established. When spectrin and actin are stripped from normal erythrocyte membrane, the membrane spontaneously disintegrates into tiny vesicles (right side-out vesicles) (Agre et al., 1985). The incorporation of exogenous spectrin into spectrin-deficient mouse erythrocytes leads to a partial correction of their fragility (Shohet, 1979). Under a stress (during an aspiration with a micropipette or under conditions of high osmotic pressure; Discher et al., 1995) vesicles are released from RBCs. The vesicles have been purified (Rumbsky et al., 1977) and contain almost no spectrin. The vesicle release seems to be a general protective mechanism of RBCs. Aging (damage accumulating) of the RBCs is accompanied by 1) a significant decrease in their volume, apparently due to vesicle release (Shinozuka, 1994), 2) an increase in their density, and 3) the formation of Heinz bodies (Schluter and Drenckhahn, 1986). The local sequestering of a damaged skeleton surface (spectrin, protein 4.1, ankyrin, etc.) associated with the formation of the Heinz bodies and hemoglobin oxidation (Jarolim et al., 1990; Liu et al., 1996) seems to be balanced by the loss of an equivalent fraction of membrane components and the cytoplasmic volume contained in the membrane vesicles. This leads us to propose that myosin II acts as a facilitating factor in these processes.

Membrane vesiculation and, as mentioned above, activation of the actomyosin II machinery in the red blood cells depend on the $[Ca^{2+}]_i$ increase. This increase (due to the decrease in Ca^{2+} active transport; Seidler and Swislocki, 1991) is involved in aging of the RBCs and induces the separation of the membrane skeleton from the lipidic bilayer and the vesiculation of the membrane (inside-out vesicles) (Allan and Michell, 1978; Ponnappa et al., 1980; Leibler, 1986; Lombardo and Low, 1994). The curvature of the lipid bilayer involved in the vesiculation is controlled by the ionic gradient across the membrane (monovalent and divalent ions) (Henseleit et al., 1990; Backer and Dawidowicz, 1987). The vesiculation mechanism was described in the case of the experimental formation of the inside-out vesicles of erythrocyte ghosts (Lew et al., 1988).

We have qualitatively tested the consequence of the local $[Ca^{2+}]_i$ increase for the activation of the myosin II machinery through the phosphorylation of myosin II regulatory light chains by myosin light chain kinase. We used autoradiograms of the sodium dodecyl sulfate polyacrylamide gel electrophoresis patterns of the whole proteins of ^{32}P-labeled RBCs, at rest or submitted to high shear stress. We used an ectacytometer for this purpose (Bessis and Mohandas, 1975); the shear stress was increased up to the appearance of slight hemolysis. Because of the low intracellular amount of myosin II, only qualitative phosphorylation of these light chains may be observed (unpublished results). The study of the actomyosin II machinery during the shear stress should validate the facilitating function of myosin II in the red blood cell repair that we propose and its corollary, the presence of a low amount of myosin II in the mass of the Heinz bodies.

We thank Drs. J. Chenevert and M. Marden for correction of the English manuscript.

This work was supported by Institut Jacques Monod, UMR 7592, CNRS Universités Paris VI and Paris VII, 2 place Jussieu, F-75005 Paris, and URA671, CNRS Station de Zoologie Marine, BP28 F-06234 Villefranche-sur-Mer Cedex.

REFERENCES

Adamo, H. P., A. F. Rega, and P. J. Garrahan. 1990. The E2 in equilibrium E1 transition of the Ca^{2+}-ATPase from plasma membranes studied by phosphorylation. *J. Biol. Chem.* 265:3789–3792.

Agre, P., J. F. Casella, W. H. Zinkham, C. McMillan, and V. Bennet. 1985. Partial deficiency of erythrocyte spectrin in hereditary spherocytosis. *Nature.* 314:380–383.

Albritton, E. C. 1952. Standard Values in Blood. Saunders Company, Philadelphia and London.

Allan, D., and R. Michell. 1978. A calcium activated polyphosphoinositide phosphodiesterase in the plasma membrane of human and rabbit erythrocytes. *Biochim. Biophys. Acta.* 508:277–286.

Backer, J. M., and E. A. Dawidowicz. 1987. Restoration of phospholipid flippase from rat liver microsomes. *Nature.* 327:341–343.

Bement, W., P. Forscher, and M. Mooseker. 1993. A novel cytoskeletal structure involved in purse string wound closure and cell polarity maintenance. *J. Cell Biol.* 121:565–578.

Bennett, V. 1985. The membrane skeleton of human erythrocytes and its implications for more complex cells. *Annu. Rev. Biochem.* 54:273–304.

Bennett, V., and D. Branton. 1977. Selective association of spectrin with the cytoplasmic surface of human erythrocyte plasma membranes. *J. Biol. Chem.* 252:2753–2763.

Bennett, V., and P. Stenbuck. 1980. Association between ankyrin and the cytoplasmic domain of band-3 isolated from human erythrocyte membrane. *J. Biol. Chem.* 255:6424–6432.

Bessis, M., and N. Mohandas. 1975. A diffractometric method for the measurements of cellular deformability. *Blood Cells.* 1:307–313.

Bloch, R., and D. Pumplin. 1992. A model of spectrin as a concertina in the erythrocyte membrane skeleton. *Trends Cell Biol.* 7:186–189.

Boal, D. H. 1994. Computer simulation of a model network for the erythrocyte cytoskeleton. *Biophys. J.* 67:521–529.

Branton, D., C. Cohen, and J. Tyler. 1981. Interaction of cytoskeletal proteins of human erythrocyte membrane. *Cell.* 24:24–32.

Chrzanowska-Wodnicka, M., and K. Burridge. 1996. Rho-stimulated contractility drives the formation of stress fibers and focal adhesions. *J. Cell Biol.* 133:1403–1415.

Colin, F. C., and S. L. Schrier. 1991. Myosin content and distribution in human neonatal erythrocytes are different from adult erythrocytes. *Blood.* 78:3052–3055.

Daniels, R., M. McKay, E. Atkinson, and A. Hipkiss. 1983. Subcellular distribution of abnormal proteins in rabbit reticulocytes. Effects of cellular maturation, phenylhydrazine and inhibitors of ATP synthesis. *FEBS Lett.* 156:145–150.

Der Terrossian, E., C. Deprette, I. Lebbar, and R. Cassoly. 1994. Purification and characterization of erythrocyte caldesmon. *Eur. J. Biochem.* 219:503–511.

Discher, D. E., R. Winardi, P. O. Schischmanoff, M. Parra, J. G. Conboy, and N. Mohandas. 1995. Mechanochemistry of protein-4.1's spectrin-actin-binding domain: ternary complex interactions, membrane binding, network integration, structural strengthening. *J. Cell Biol.* 130:897–907.

Elgsaeter, A., B. T. Stokke, A. Mikkelsen, and D. Branton. 1986. The molecular basis of erythrocyte shape. *Science.* 234:1217–1223.

Foder, B., and O. Scharff. 1981. Decrease of apparent calcmodulin affinity of erythrocytes Ca^{2+}-Mg^{2+}-ATPase at low Ca^{2+} concentrations. *Biochim. Biophys. Acta.* 649:367–376.

Fowler, V. 1986. An actomyosin contractile mechanism for erythrocyte shape transformations. *J. Cell. Biochem.* 31:1–9.

Fowler, V. M. 1996. Regulation of actin filament length in erythrocytes and striated muscle. *Curr. Opin. Cell Biol.* 8:86–96.

Fowler, V., and V. Bennett. 1984. Erythrocyte membrane tropomyosin: purification and properties. *J. Biol. Chem.* 259:5978–5989.

Fowler, V., J. Davis, and V. Bennett. 1985. Human erythrocyte myosin: identification and purification. *J. Cell Biol.* 100:47–55.

Fukushima, Y., and H. Kon. 1990. On the mechanism of loss of deformability in human erythrocytes due to Heinz body formation: a flow EPR study. *Toxicol. Appl. Pharmacol.* 102:205–218.

Gardner, K., and V. Bennett. 1986. A new erythrocyte membrane associated protein with calmodulin binding activity. Identification and purification. *J. Biol. Chem.* 261:1339–1348.

Graf, E., and J. Penniston. 1981. Equimolar interaction between calmodulin and the Ca^{2+}-ATPase from human erythrocyte membrane. *Arch. Biochem. Biophys.* 210:257–262.

Gratzer, W. 1981. The red cell membrane and its cytoskeleton. *Biochem. J.* 198:1–8.

Hansen, J. C., R. Skalak, S. Chien, and A. Hoger. 1997. Influence of network topology on the elasticity of the red blood cell membrane skeleton. *Biophys. J.* 72:2369–2381.

Henseleit, U., G. Plasa, and C. Haest. 1990. Effects of divalent cations on lipid flip-flop in the human erythrocyte membrane. *Biochim. Biophys. Acta.* 1029:127–135.

Higashihara, M., D. J. Hartshorne, R. Craig, and M. Ikebe. 1989. Correlation of enzymatic properties and conformation of bovine erythrocytes myosin. *Biochemistry.* 28:1642–1649.

Ikebe, M., and S. Reardon. 1990. Phosphorylation of smooth muscle myosin light chain kinase by smooth muscle Ca^{2+}-CaM dependent multifunctional protein kinase. *J. Biol. Chem.* 265:8975–8978.

Jarolim, P., M. Lahav, S. C. Liu, and J. Palek. 1990. Effect of hemoglobin oxidation products on the stability of red cell membrane skeletons and the associations of skeletal proteins: correlation with a release of hemin. *Blood.* 76:2125–2131.

Johnson, R., and K. Tang. 1992. Induction of a Ca^{++} activated K^+ channel in human erythrocytes by mechanical stress. *Biochem. Biophys. Acta.* 1107:314–318.

Knipper, M., U. Zimmerman, I. Köpschall, K. Rohbock, S. Jüngling, and H. Zenner. 1995. Immunological identification of candidate proteins involved in regulating active shape changes of outer hair cells. *Hearing Res.* 86:100–110.

Kodicek, M., J. Syttnar, L. Micevova, and T. Marik. 1990. Red blood cells under mechanical stress. *Gen. Physiol. Biophys.* 9:291–299.

Kosk-Kosicka, D., and T. Bzdega. 1988. Activation of the erythrocyte Ca^{2+}-ATPase by either self-association or interaction with calmodulin. *J. Biol. Chem.* 263:18124–18129.

Kozlov, M. M., L. V. Chernomordik, and V. S. Markin. 1990. A mechanism of formation of protein-free regions in the red cell membrane: the rupture of the membrane skeleton. *J. Theor. Biol.* 144:347–365.

Larsen, F., S. Katz, B. Roufogalis, and D. Brooks. 1981. Physiological shear stresses enhances the calcium permeability of human erythrocytes. *Nature.* 294:667–668.

Leibler, S. 1986. Curvature instability in membrane. *J. Physique.* 47: 507–516.

Leverett, L., J. Hellums, P. Alfrey, and E. Lynch. 1972. Red blood cell damage by shear stress. *Biophys. J.* 12:257–273.

Lew, V., A. Hockaday, C. Freeman, and R. Boockin. 1988. Mechanism of spontaneous inside-out vesiculation of red cell membranes. *J. Cell Biol.* 106:1893–1901.

Liu, S. C., L. H. Derick, and J. Palek. 1993. Dependence of the permanent deformation of red blood cell membranes on spectrin dimer-tetramer equilibrium: implication for permanent membrane deformation of irreversibly sickled cells. *Blood.* 81:522–528.

Liu, S.-C., S. J. Yi, J. R. Mehta, P. E. Nichols, S. K. Ballas, P. W. Yacono, D. E. Golan, and J. Palek. 1996. Red cell membrane remodeling in sickle cell anemia. Sequestration of membrane lipids and proteins in Heinz bodies. *J. Clin. Invest.* 97:29–36.

Lombardo, C. R., and P. S. Low. 1994. Calmodulin modulates protein-4.1 binding to human erythrocyte membranes. *Biochim. Biophys. Acta.* 1196:139–144.

Lundberg, S., V.-P. Lehto, and L. Backman. 1992. Characterization of calcium binding to spectrins. *Biochemistry.* 31:5665–5671.

Marchesi, V. T. 1985. Stabilizing infrastructure of cell membranes. *Annu. Rev. Cell Biol.* 1:531–561.

Marston, S., and C. Redwood. 1993. The essential role of tropomyosin in cooperative regulation of smooth muscle thin filament activity by caldesmon. *J. Biol. Chem.* 268:12317–12320.

Matovcick, M., U. Gröschel-Stewart, and S. Schrier. 1986. Myosin in adult and neonatal human erythrocyte membranes. *Blood.* 67:1668–1674.

Milos, M., J. Shaer, M. Comte, and J. Cox. 1986. Calcium-proton and calcium-magnesium antagonisms in calmodulin. Microcalorimetric and potentiometric analyses. *Biochemistry.* 25:6279–6287.

Niggli, V., E. Adunyah, J. Penniston, and E. Carafoli. 1981. Purified (Ca^{2+}-Mg^{2+})-ATPase of erythrocyte membrane. Restoration and effect of calmodulin and phospholipids. *J. Biol. Chem.* 256:395–401.

Ogawa, Y., and M. Tanokura. 1984. Calcium binding to calmodulin: effects of ionic strength, Mg^{2+}, pH and temperature. *J. Biochem.* 95: 19–28.

Pekrun, A., J. C. Pinder, S. A. Morris, and W. B. Gratzer. 1989. Composition of the ternary protein complex of the red cell membrane cytoskeleton. *Eur. J. Biochem.* 182:713–717.

Ponnappa, P., A. Greenquist, and S. Shohet. 1980. Calcium-induced changes in poly-phosphoinositides and phosphatidate in normal erythrocytes, sickle cells and hereditary pyropoikilocytes. *Biochim. Biophys. Acta.* 598:494–501.

Racusen, R. H., and G. R. Pasternack. 1990. Microscale, filtration-type binding assay for studying myosin-erythrocyte protein-4.1 interactions. *Anal. Biochem.* 188:344–348.

Rumbsky, M. G., J. Trotter, D. Allan, and R. H. Michell. 1977. Recovery of membrane micro-vesicles from human erythrocytes stored for transfusion: a mechanism for the erythrocyte discocyte-to-spherocyte shape transformation. *Biochem. Soc. Trans.* 5:126–128.

Sackett, D., and D. Kosk-Kosicka. 1996. The active species of plasma membrane Ca^{2+}-ATPase are dimer and monomer-calmodulin complex. *J. Biol. Chem.* 271:9987–9991.

Saxton, M. 1995. Single-particle tracking: effects of corrals. *Biophys. J.* 69:389–398.

Saxton, M. J. 1992. Gaps in the erythrocyte membrane skeleton: a stretched net model. *J. Theor. Biol.* 155:517–536.

Schluter, K., and D. Drenckhahn. 1986. Co-clustering of denatured hemoglobin with band 3: its role in binding of autoantibodies against band 3 to abnormal and aged erythrocytes. *Proc. Natl. Acad. Sci. USA.* 83: 6137–6141.

Schrier, S., B. Hardy, I. Junga, and L. Ma. 1981. Actin activated ATPase in human red cell membranes. *Blood.* 58:953–962.

Seidler, N. W., and N. I. Swislocki. 1991. Ca^{2+} transport activities of inside-out vesicles prepared from density-separated erythrocytes from rat and human. *Mol. Cell. Biochem.* 105:159–169.

Shen, B. W., R. Josephs, and T. L. Steck. 1986. Ultrastructure of the intact skeleton of the human erythrocyte membrane. *J. Cell Biol.* 102: 997–1006.

Shinozuka, T. 1994. Changes in human red blood cells during ageing in vivo. *Keio J. Med.* 43:155–163.

Shohet, S. 1979. Restoration of spectrin deficient spherocytic mouse erythrocyte membranes. *J. Clin. Invest.* 64:483–494.

Shohet, S., and N. Mohandas. 1988. Red Cell Membranes. Churchill-Livingston, New York.

Sinard, J. H., W. F. Stafford, and T. D. Pollard. 1989. The mechanism of assembly of *Acanthamoeba* myosin-II minifilaments: minifilaments assemble by three successive dimerization steps. *J. Cell Biol.* 109: 1537–1547.

Solar, I., J. Dulitzky, and N. Shaklai. 1990. Hemin-promoted peroxidation of red cell cytoskeletal proteins. *Arch. Biochem. Biophys.* 283:81–89.

Speicher, D. W., L. Weglarz, and T. M. DeSilva. 1992. Properties of human red cell spectrin heterodimer (side-to-side) assembly and identification of an essential nucleation site. *J. Biol. Chem.* 267:14775–14782.

Steck, T., and J. Kant. 1974. Preparation of impermeable ghost and inside-out vesicles from erythrocyte membranes. *Methods Enzymol.* 31:172–180.

Tan, J. L., S. Ravid, and J. A. Spudich. 1992. Control of nonmuscle myosins by phosphorylation. *Annu. Rev. Biochem.* 61:721–759.

Tanaka, T., K. Kadowaki, E. Lazarides, and K. Sobue. 1991. Ca^{2+} dependent regulation of the spectrin/actin interaction by calmodulin and protein-4.1. *J. Biol. Chem.* 266:1134–1140.

Tchernia, G., N. Mohandas, and S. B. Shohet. 1981. Deficiency of skeletal membrane protein band 4.1 in homozygous hereditary elliptocytosis. *J. Clin. Invest.* 68:454–460.

Trybus, K. 1991. Regulation of smooth muscle myosin. *Cell Motil. Cytoskel.* 18:81–85.

Van Buren, P., W. Guilford, G. Kennedy, J. Wu, and D. Warshaw. 1995. Smooth muscle myosin: a high force generating molecular motor. *Biophys. J.* 68:256s–259s.

Waugh, R. E. 1983. Effects of abnormal cytoskeletal structure on the erythrocyte membrane mechanical properties. *Cell Motil. Cytoskel.* 3:609–622.

Waugh, S., and P. Low. 1985. Hemichrome binding to band 3: nucleation of Heinz bodies on the erythrocyte membrane. *Biochemistry.* 24:34–39.

Waugh, S., B. Willardson, R. Kannan, R. Labotka, and P. Low. 1986. Heinz bodies induce clustering of band 3, glycophorin, and ankyrin in sickle cell erythrocytes. *J. Clin. Invest.* 78:1155–1160.

Wong, A. J., D. P. Kiehart, and T. D. Pollard. 1985. Myosin from human erythrocytes. *J. Biol. Chem.* 260:46–49.

Yoshino, H., and O. Minari. 1991. Characterization of the lateral interaction between erythrocyte spectrin subunits. *J. Biochem.* 110:553–558.